HHS Public Access

Author manuscript

J Allergy Clin Immunol. Author manuscript; available in PMC 2021 July 30.

Published in final edited form as:

J Allergy Clin Immunol. 2021 January ; 147(1): 309–320.e6. doi:10.1016/j.jaci.2020.04.033.

Efficacy and safety of anti-CD45–saporin as conditioning agent for RAG deficiency

Maria Carmina Castiello, PhD[a,b,*], **Marita Bosticardo, PhD**[c,*], **Nicolò Sacchetti, PhD**[a], **Enrica Calzoni, MD**[a,c], **Elena Fontana, PhD**[b,d], **Yasuhiro Yamazaki, MD, PhD**[c], **Elena Draghici, BS**[a], **Cristina Corsino**[c], **Ileana Bortolomai, PhD**[a], **Lucia Sereni, PhD**[a], **Hsin-Hui Yu, MD, PhD**[c], **Paolo Uva, PhD**[e], **Rahul Palchaudhuri, PhD**[f,g,h], **David T. Scadden, MD**[f,g], **Anna Villa, MD**[a,b], **Luigi D. Notarangelo, MD**[c]

[a]San Raffaele Telethon Institute for Gene Therapy SR-Tiget, IRCCS San Raffaele Scientific Institute, Milan

[b]Institute of Genetic and Biomedical Research Milan Unit, National Research Council, Milan

[c]Laboratory of Clinical Immunology and Microbiology, Division of Intramural Research, National Institute of Allergy and Infectious Diseases, National Institutes of Health, Bethesda

[d]Human Genome Lab, Humanitas Clinical and Research Center, Milan

[e]CRS4, Science and Technology Park Polaris, Pula

[f]Department of Stem Cell and Regenerative Biology, Harvard University, Harvard Stem Cell Institute, Cambridge

[g]Center for Regenerative Medicine, Massachusetts General Hospital, Boston

[h]Magenta Therapeutics, Cambridge

Abstract

Background: Mutations in the recombinase-activating genes cause severe immunodeficiency, with a spectrum of phenotypes ranging from severe combined immunodeficiency to immune dysregulation. Hematopoietic stem cell transplantation is the only curative option, but a high risk of graft failure and poor immune reconstitution have been observed in the absence of myeloablation.

Objectives: Our aim was to improve multilineage engraftment; we tested nongenotoxic conditioning with anti-CD45 mAbs conjugated with saporin CD45 (CD45-SAP).

Methods: *Rag1-KO* and *Rag1-F971L* mice, which represent models of severe combined immune deficiency and combined immune deficiency with immune dysregulation, respectively, were

Corresponding author: Anna Villa, MD, SR-Tiget, Via Olgettina 58, Milan, 20127, Italy. villa.anna@hsr.it. Or: Luigi D. Notarangelo, MD, Immune Deficiency Genetics Section, Laboratory of Clinical Immunology and Microbiology, National Institute of Allergy and Infectious Diseases, National Institutes of Health, Building 10, Room 5-3950, 10 Center Drive, Bethesda, MD 20892. luigi.notarangelo2@nih.gov.

*These authors are co-first authors.

Disclosure of potential conflict of interest: The authors declare that they have no relevant conflicts of interest.

conditioned with CD45-SAP, CD45-SAP plus 2 Gy of total body irradiation (TBI), 2 Gy of TBI, 8 Gy of TBI, or no conditioning and treated by using transplantation with lineage-negative bone marrow cells from wild-type mice. Flow cytometry and immunohistochemistry were used to assess engraftment and immune reconstitution. Antibody responses to 2,4,6-trinitrophenyl–conjugated keyhole limpet hemocyanin were measured by ELISA, and presence of autoantibody was detected by microarray.

Results: Conditioning with CD45-SAP enabled high levels of multilineage engraftment in both *Rag1* mutant models, allowed overcoming of B- and T-cell differentiation blocks and thymic epithelial cell defects, and induced robust cellular and humoral immunity in the periphery.

Conclusions: Conditioning with CD45-SAP allows multilineage engraftment and robust immune reconstitution in mice with either null or hypomorphic *Rag* mutations while preserving thymic epithelial cell homeostasis.

Graphical Abstract

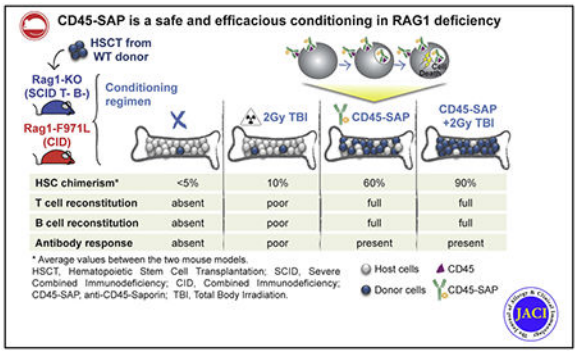

Keywords

RAG deficiency; conditioning; anti-CD45–saporin; immunotoxin; engraftment; immune reconstitution; hematopoietic stem cell transplantation; thymic epithelial cells

Severe combined immune deficiency (SCID) includes various inherited immune disorders characterized by severe lymphopenia and lack of adaptive immunity.[1–3] Over the past decade, allogeneic hematopoietic stem cell transplantation (HSCT) and gene correction of autologous stem cell precursors have achieved substantial success in treating patients with SCID thanks to newborn screening and improvement in donor selection, transplant protocols, and critical care.[4–6]

For patients with SCID, the use of preparative regimens aimed at facilitating the engraftment of donor-derived hematopoietic stem cells (HSCs) continues to be controversial because T-cell reconstitution from a pool of committed lymphoid progenitors is also observed in the absence of durable HSC engraftment. Without conditioning, however, a higher risk of graft rejection and poor T- and B-cell reconstitution have been reported for patients with recombinase-activating gene (*RAG*) mutations, especially after haploidentical HSCT.[5,7] In addition to natural killer cell–mediated rejection of donor cells, it has been hypothesized that poor immune reconstitution may also reflect competition between autologous and donor

cells at early stages of T- and B-cell development that precede expression of the *RAG* genes.[7–9] It has been demonstrated that the use of preparative regimens for HSCT in *RAG*-deficient patients is associated with a lower risk of treatment failure and superior T- and B-cell reconstitution than is no conditioning.[5] However, conditioning regimens may cause acute and chronic toxicity, including organ damage, risk of infections, and infertility.[10] These considerations are particularly important for *RAG* deficiency manifesting as combined immunodeficiency with immune dysregulation (CID-ID), in which the unusual clinical presentation often leads to delayed diagnosis and progressive development of organ damage.[11–13] In these patients, the mortality rate reported after HSCT is higher than the rate observed in patients with typical or atypical SCID.[13] Overall, these observations emphasize the need to develop nongenotoxic conditioning regimens. Recently, biologic approaches based on mAbs specifically targeting hematopoietic stem and progenitor cells (HSPCs) have been developed. The use of anti-CD117 mAb has been shown to efficiently condition immunocompetent mice, enabling the engraftment of donor cells,[14–16] and a clinical trial is under way in patients with SCID (ClinicalTrials.gov identifier NCT02963064). However, although CD117-SAP represents a promising nonmyeloablative agent as it depletes autologous HSPCs while preserving host immunity,[17–19] its use may not suffice in the context of CID-ID, in which there is a specific need to eliminate autoreactive host cells. For this reason, because of their ability to eliminate both precursor and mature hematopoietic cells (as they all express CD45), anti-CD45 mAbs represent a more attractive target for the conditioning of patients with CID-ID. Indeed, lytic anti-CD45 mAbs have been tested in patients with hematologic malignancies,[20] and promising results have been observed even in a RAG1-deficient patient with immune dysregulation.[21] Conjugation of anti-CD45 mAb with saporin, a ribosome-inactivating protein that lacks the cell entry domain and is toxic only on receptor-mediated internalization,[22] results in an immunotoxin (anti-CD45 mAb conjugated with saporin [CD45-SAP]) that efficiently depletes HSCs in wild-type (WT) mice, enabling stable multilineage engraftment with minimal organ toxicity.[23] However, it is not known whether these innovative immunotoxin-based conditionings are effective in immunodeficient models in which bone marrow (BM) and thymus niches are occupied by autologous mutant T- and B- progenitor cells.

This is of special concern for patients whose hypomorphic mutations cause both immunodeficiency and severe immune dysregulation. Murine models recapitulating the spectrum of phenotypes associated with *RAG* mutations in humans may represent a useful tool to test such novel therapeutic approaches. We have recently described newly generated mouse models carrying missense mutations in the RAG1 carboxy-terminal domain, permitting partial T- and B-cell development and recapitulating the phenotype observed in patients with CID-ID.[24] Here we report the effect of conditioning with CD45-SAP immunotoxin alone or combined with low-dose (2-Gy) total body irradiation (TBI) in 2 mouse models of *RAG* deficiency: the *Rag1-KO* mice,[25] mimicking SCID, and the *Rag1*-mutant mice carrying a homozygous F971L mutation (*Rag1-F971L*),[24] recapitulating CID-ID.

METHODS

Mice

C57B1/6 WT mice were purchased from Charles River Laboratories, Inc (Calco, Italy, and Wilmington, Mass). *B6.129S7-Rag.1*$^{t1Mom/J}$ mice (referred to as *Rag1-KO*), purchased from The Jackson Laboratory, were maintained in specific pathogen–free conditions, with experimental procedures approved by the institutional animal care and use committee of San Raffaele Hospital (protocol 910). *Rag1*$^{F971L/F971L}$ (referred to as *Rag1-F971L*) mice[24] were studied according to protocol ASP LCIM6E, which was approved by the National Institute of Allergy and Infectious Diseases animal care and use committee.

Conditioning and transplantation protocols

Lineage-negative (Lin^-) cells were isolated as described[26] from 6- to 10-week-old donor CD45.1 WT mice and intravenously administered at a dose of 0.5×10^6 cells on the day of transplantation (day 0). Lin^- cell purity (>90%) was assessed by flow cytometry. The CD45-SAP immunotoxin was prepared as described[23] by combining a biotinylated anti-CD45.2 antibody (clone 104, Biolegend, San Diego, Calif) with streptavidin-SAP conjugate (Advanced Targeting Systems, San Diego, Calif) in a 1:1 molar ratio. Groups of CD45.2 *Rag1-KO* and *Rag1-F971L* recipient mice were conditioned by using the following regimens: (1) lethal (8-Gy) TBI at day −1, (2) low-dose TBI (2 Gy) at day −1, (3) intravenous injection of CD45-SAP (3 mg/kg) at day −8, and (4) CD45-SAP (3 mg/kg) at day −8 and 2 Gy of TBI at day −1. The mice were followed until 16 weeks or 21 weeks after transplantation and then humanely killed. The levels of the liver enzymes alanine aminotransferase and aspartate aminotransferase were measured as described in the Methods section of the Online Repository (at www.jacionline.org).

In vivo immunization and antibody response

In vivo challenge with the T-dependent antigen 2,4,6-trinitrophenyl (TNP)-conjugated keyhole limpet hemocyanin was performed 4 months after transplantation as previously described.[26] TNP-specific antibody titers were measured in serum by ELISA (see the Methods section of the Online Repository). Plasma levels of total IgG, IgM, and IgA were measured by using a multiplex assay (Beadlyte Mouse Immunoglobulin Isotyping kit [Millipore, Burlington, Mass]) on a Luminex Magpix instrument (Luminex Corp, Austin, Tex). Serum IgG autoantibodies were measured by using a microarray platform as described in the Methods section of the Online Repository.

Flow cytometry and TEC isolation

Single-cell suspensions were obtained from BM, spleen, thymus, and peripheral blood (PB) and stained with mAbs listed in Table E1. Samples were acquired on a FACSCanto II system (BD Biosciences, San Jose, Calif).

Thymic epithelial cells (TECs) were isolated as previously described[27] and analyzed as described in the Methods section of the Online Repository.

Histology

Thymus samples were formalin-fixed and paraffin-embedded. Sections (1.5-μm) were stained with hematoxylin and eosin. Digital images were acquired with an Olympus DP70 camera mounted on an Olympus BX60 microscope by using CellF Imaging software (Soft Imaging System GmbH, Munster, Germany). Morphometric analysis of the medullary-to-cortical ratio was evaluated by using Image-Pro software.

Statistical analyses

All results are expressed as medians plus or minus SDs. Statistical significance was assessed by using a 2-tailed Mann-Whitney test for comparing 2 groups or 1-way ANOVA and the Kruskal-Wallis test corrected for multiple comparisons by controlling false discovery rate. Statistically significant *P* values are shown in the figures as follows: **P* <.05; ***P* < .005; ****P* <.0005; *****P* <.0001.

RESULTS

Conditioning is required in null and hypomorphic *Rag1* mice

HSCT without conditioning in *RAG*-deficient patients is associated with poor immune reconstitution, possibly reflecting competition between autologous and donor-derived stem and lymphoid progenitor cells.[5,7] To assess whether the BM niches of *Rag1*-null and *Rag1-F971L* mice are receptive to donor stem cell engraftment in the absence of depletion of autologous HSPCs, we transplanted BM Lin^- cells from C57BL/6 CD45.1 WT mice into unconditioned C57BL/6 CD45.2 *Rag1-KO* and *Rag1-F971L* mice. The proportions of donor-derived $CD11b^+$ myeloid cells in the PB (Fig 1, A) and Lin^- $Sca1^+$ $c\text{-}kit^+$ (LSK) $CD48^-$ $CD150^+$ HSCs in the BM (Fig 1, B) were very low (<5%) in all *Rag1*-mutant recipient mice after the transplant procedure. To verify whether these low proportions of donor cell engraftment could nonetheless permit immune reconstitution, we analyzed the immune cell composition in central and peripheral lymphoid organs. *Rag1*-mutant mice treated by unconditioned HSCT did not reverse the B- and T-cell differentiation blocks in the BM (Fig 1, C) and thymus (Fig 1, D), respectively. In particular, the distribution of B-cell subsets in unconditioned mice was superimposable to the pattern observed in untreated *Rag1*-mutant mice, with a significant increase in the proportion of $B220^{low}$ $CD43^-$ IgM^- pre-B cells as compared with what was observed in WT mice (Fig 1, C [*left panel*]). Furthermore, in both models the absolute count of immature B cells remained significantly lower than in WT mice (Fig 1, C [*right panel*]). Thymopoiesis remained blocked at the $CD4^-$ $CD8^-$ double-negative (DN) stage in *Rag1-KO* mice on unconditioned transplantation (Fig 1, D). Untreated *Rag1-F971L* mice showed residual capacity to generate double-positive and single-positive (SP) cells (Fig 1, D [*left panel*]), and only a modest increase in their proportion was observed after unconditioned HSCT (Fig 1, D).

The peripheral reconstitution mirrored that observed in central organs, with low white blood cell (WBC) counts measured over time in the PB of both *Rag1*-mutant strains on unconditioned HSCT (Fig 1, E). Four months after unconditioned transplantation, the absolute number of $CD19^+$ $B220^+$ B cells in the spleen of *Rag1*-mutant mice was no different from the values observed in untreated mice, but it was significantly lower than in

WT mice (Fig 1, F). Moreover, flow cytometric analysis of splenic B-cell subsets showed that unconditioned HSCT did not induce amelioration in the distribution of transitional ($CD19^+$ $B220^+$ $CD21^{intermediate/low}$ $CD24^{high}$), follicular ($CD19^+$ $B220^+$ $CD21^{intermediate}$ $CD24^{low}$), and marginal zone (MZ) ($CD19^+$ $B220^+$ $CD21^{high}$ $CD24^{intermediate}$) B cells (Fig 1, G). Similarly, the T-cell counts remained 50- to 100-fold lower in mouse models both with and without transplantation than in untreated WT mice (Fig 1, H). Phenotypic analysis of splenic T-cell subsets did not reveal any difference in the proportion of naive ($CD62L^+$ $CD44^-$) and effector/memory ($CD62L^{-/+}$ $CD44^+$) $CD4^+$ (Fig 1, I) and $CD8^+$ (Fig 1, J) cells between untreated and unconditioned *Rag1*-mutant mice that received transplants.

Altogether, these data demonstrate that in the absence of conditioning, MHC-matched HSCT into *Rag1*-deficient hosts does not enable effective engraftment of donor-derived hematopoietic and progenitor cells and does not correct the immune deficiency, indicating the need to deplete HSPCs.

CD45-SAP induces efficient depletion of endogenous HSCs in *Rag1*^{mutant} mice

To test whether conditioning with CD45-SAP can efficiently deplete endogenous HSPCs from the BM and thymus, we injected *Rag1*-mutant mice with the CD45-SAP immunotoxin,[23] alone or in combination with low-dose (2-Gy) TBI, and compared the results with those obtained with 2 Gy or 8 Gy of TBI. CD45-SAP–based conditioning regimens were well tolerated in both *Rag1*-mutant mice (see Fig E1, A in the Online Repository at www.jacionline.org). After they had been humanely killed, necropsy did not show macroscopic alterations in their organs; in addition, normal serum levels of aminotransferase enzymes were observed in the majority of treated *Rag1*-mutant mice. Only a few mice showed a modest increase in alanine aminotransferase and aspartate aminotransferase levels, suggesting mild liver toxicity on conditioning with CD45-SAP (see Fig E1, B and C). To assess the degree of HSC depletion, we evaluated the absolute counts of LSK cells (which comprise both HSCs and progenitor cells) and LSK $CD48^-$ $CD150^+$ HSCs in the BM of *Rag1*-mutant mice 8 days after CD45-SAP administration or 1 day after irradiation (see Fig E2, A in the Online Repository at www.jacionline.org). A single dose of CD45-SAP immunotoxin resulted in the depletion of 85.9% and 76.3% of LSK cells in *Rag1-KO* and *Rag1-F971L* mice, respectively (Fig E, 2B). Even higher levels of depletion were observed in the HSC compartment (95.2% in *Rag1-KO* and 91.7% in *Rag1-F971L* mice) (see Fig E2, C). Use of low-dose TBI was associated with significant variability in the depletion of HSCs in both models (see Fig E2, C). Of note, the combination of CD45-SAP with 2 Gy of TBI displayed a synergistic effect in depleting HSCs (94.7% in *Rag1-KO* and 100% in *Rag1-F971L* mice) and progenitor cells (96.3% in *Rag1-KO* and 99.9% in *Rag1-F971L* mice) (see Fig E2, B and C) and corresponded to the highest level of depletion in both mouse models.

The kinetics of immune recovery in mice conditioned with CD45-SAP mirror donor chimerism in PB

To determine whether the degree of HSC depletion induced by CD45-SAP permits durable multilineage engraftment, we monitored the kinetics of myeloid chimerism and immune reconstitution in the PB over time by flow cytometry. As expected, low levels of myeloid chimerism were observed in both *Rag1*-mutant models on conditioning with 2 Gy of TBI,

whereas 8 Gy of TBI induced the highest levels of myeloid engraftment (see Fig E2, D and E). Conditioning with CD45-SAP alone allowed intermediate levels of myeloid chimerism in both models, but the combination of CD45-SAP and 2 Gy of TBI yielded similarly high levels of donor myeloid chimerism, as observed in 8-Gy–conditioned mice, suggesting optimal engraftment of donor-derived long-term HSCs (see Fig E2, D and E).

In parallel, we monitored the kinetics of immune reconstitution in the PB (see Fig E3, A in the Online Repository at www.jacionline.org). Irradiation with 2 Gy alone was not sufficient to normalize the WBC count or correct T- and B-cell deficiency in *Rag1*-mutant mice (see Fig E3, B–E). In contrast, *Rag1*-mutant mice that received a transplant and were conditioned with CD45-SAP plus 2 Gy of TBI or with 8 Gy showed a significant increase in WBC, T-cell, and B-cell counts already at 8 weeks after transplantation (see Fig E3, B–D). Conditioning with CD45-SAP alone resulted in slower kinetics of WBCs and lymphoid recovery, with B-cell reconstitution in particular remaining sub-optimal in both mouse models (see Fig E3, B–E).

These results indicate that conditioning with CD45-SAP plus 2 Gy of TBI promotes high levels of engraftment of donor HSPCs equivalent to what was observed with 8 Gy of TBI, and it permits a faster kinetics of immune reconstitution than either CD45-SAP or 2 Gy of irradiation alone.

CD45-SAP–based conditioning allows efficient donor chimerism and lymphopoiesis in central lymphoid organs of *Rag1*-mutant mice

To verify whether conditioning with CD45-SAP is able to create a permissive environment for stable engraftment of donor HSCs in *Rag1*-mutant mice, we analyzed the proportion of donor CD45.1$^+$ HSCs in the BM of differentially conditioned *Rag1*-mutant mice 4 months after transplantation. High levels of donor chimerism were observed in the HSC compartment of mice conditioned with 8 Gy or CD45-SAP plus 2 Gy, irrespective of the genetic background (Fig 2, A). Administration of CD45-SAP alone resulted in a partial and variable donor HSC chimerism ranging from 32.04% to 100% in *Rag1-KO* mice and from 5.02% to 86.2% in *Rag1-F971L* mutants. In contrast, 2 Gy of irradiation resulted in poor HSC engraftment in both models (Fig 2, A).

To test how conditioning affects B-cell reconstitution, we determined the proportion of donor CD45.1$^+$ WT cells at various stages of differentiation. Consistent with the levels of donor HSC chimerism, conditioning with 2 Gy of irradiation and with CD45-SAP resulted in modest or intermediate levels of donor chimerism, respectively, at the pro–B-cell stage, in which competition with autologous cells occurs (Fig 2, B). In contrast, conditioning with CD45-SAP plus 2 Gy or with 8 Gy of irradiation allowed high levels of donor chimerism already at the pro–B-cell stage. Finally, irrespective of the nature of conditioning, robust donor chimerism was detected at later stages of B-cell development, and even in *Rag1-F971L* mice, in spite of the residual capacity to generate mature B cells[24] (Fig 2, C). Immunotoxin-based regimens or 8 Gy of TBI resulted in a distribution of BM B-cell subsets that was similar to what was observed in WT mice (Fig 2, C [*left panel*]), with an absolute count of immature and recirculating mature B cells that was significantly higher than in untreated *Rag1-KO* and *Rag1-F971L* mice (Fig 2, C [*right panel*]).

In parallel, we assessed donor chimerism in the thymus at different stages of T-cell development, including early thymic progenitors, DN1 to DN4 stage cells, double-positive cells, and SP4 ($CD4^+$) and SP8 ($CD8^+$) cells. Interestingly, in both mouse models, conditioning with CD45-SAP alone or with 2Gy was associated with a fluctuation in the proportion of donor cells at early stages (DN1-4) of thymopoiesis, and low levels of donor chimerism were observed especially at the DN2-DN3 stage (Fig 3, A). In contrast, conditioning with $CD45^-$SAP plus 2 Gy or with 8 Gy permitted robust levels of donor chimerism throughout the early stages of thymopoiesis (Fig 3, A). Finally, irrespective of the conditioning used, high levels of donor chimerism were detected beyond the DN3 stage, reflecting the selective advantage provided by normal *Rag1* expression to bypass the developmental block. To better quantify the impact of conditioning and transplant on thymic output, we analyzed thymocyte counts and subset distribution when the mice were humanely killed. Both untreated *Rag1*-mutant models were characterized by a dramatic reduction in total thymocyte counts (Fig 3, B). Thymic output was corrected in the mice conditioned with CD45-SAP alone or in combination with 2 Gy and with 8 Gy of irradiation (Fig 3, B), with rescue of early and late thymopoiesis (Fig 3, C) in both mouse models. Conversely, 2 Gy of TBI only partially restored thymocyte counts (Fig 3, B) and T-cell subset distribution (Fig 3, C) in both mouse models.

CD45-SAP conditioning supports the reconstitution of epithelial cells in the thymus of *Rag1*-mutant mice

To test the effect of conditioning on thymic epithelial architecture, whole thymic structures were analyzed by histology, and in parallel the proportions of medullary TECs (mTECs) and cortical TECs were assessed by flow cytometry. Conditioning with CD45-SAP–based regimens allowed restoration of normal thymus morphology with clear demarcation of medullary and cortical areas and normalization of the medullary-to-cortical ratio (Fig 4, A and B in the Online Repository at www.jacionline.org). Conversely, poor reconstitution of the thymic epithelial compartment was observed in *Rag1*-mutant mice conditioned with 2 Gy of irradiation alone (Fig 4, A and B). Flow cytometric analysis further demonstrated that in *Rag1-KO* mice CD45-SAP–based regimens were more effective than irradiation-only–based regimens in increasing the frequency of mTECs (Fig 4, C). Overall, reconstitution of the mTEC compartment was more robust in *Rag1-F971L* than in *Rag1-KO* mice, irrespective of the conditioning used (Fig 4, C).

Altogether, these findings indicate that conditioning with CD45-SAP, alone or in combination with 2 Gy of TBI, permits reconstitution of both thymocyte and TEC compartments.

Correction of peripheral lymphoid organ abnormalities in *Rag1*-mutant mice on conditioning with CD45-SAP–based regimens

Next, we assessed the immunologic reconstitution by analyzing the T- and B-cell compartment in the spleen of *Rag1*-mutant mice 4 months after transplantation. As expected, because of the strong selective advantage of WT-derived cells in generating mature T and B lymphocytes, the splenic T- and B-cell compartments of *Rag1-KO* mice that had received a transplant were composed entirely of $CD45.1^+$ donor-derived cells in all

conditioning groups (Fig 5, A). In *Rag1-F971L* mice, a small proportion of host-derived T and B cells was observed on conditioning with CD45-SAP alone, with CD45-SAP plus 2 Gy, or with 2 Gy (Fig 5, A). The levels of myeloid engraftment in the spleen paralleled those found in the PB (see Fig E2, D and E) and in HSCs (see Fig E2, C).

In both *Rag1*-mutant models, irrespective of the conditioning used, transplantation resulted in an increase in the splenic T-cell counts, as compared with in untreated mice, although the total T-cell count remained lower than in WT mice (Fig 5, B). To exclude the possibility that the increase of T-cell counts after transplantation may reflect homeostatic proliferation in a T-cell lymphopenic environment, we evaluated the distribution of naive and effector/memory T cells. As previously demonstrated,[24] hypomorphic *Rag1-F971L* mice have a significant decrease in the proportion of naive T cells (Fig 5, C) as compared with that in WT mice and a relative increase in the proportion of effector/memory T cells (Fig 5, C). After transplantation, a similar distribution of naive and effector/memory $CD4^+$ and $CD8^+$ cells was observed in both *Rag1*-mutant models as compared with in WT mice, with the exception of *Rag1-KO* mice conditioned with low-dose irradiation (Fig 5, C). Similarly, improved B-cell reconstitution was observed in both models as compared with that in their respective untreated controls, although in all conditions B-cell count was lower than in WT mice (Fig 5, D). In both models, the relative distribution of transitional, follicular, and MZ B cells approached what was observed in WT mice, in particular, in mice conditioned with CD45-SAP–based regimens or with 8 Gy of TBI (Fig 5, E). In contrast, 2 Gy of TBI was associated with a poorer B-cell count, a relative excess of MZ B cells, and a lower proportion of follicular B cells, especially in *Rag1*-KO mice (Fig 5, D and E).

Conditioning with CD45-SAP allows correction of adaptive immune responses in *Rag1*-mutant mice that received a transplant

Rag1-KO and *Rag1-F971L* mice are characterized by lack and variable levels of serum immunoglobulins, respectively.[24,25] Compared with untreated mice, the *Rag1-KO* mice that received a transplant had significantly higher IgM and IgG serum levels that were within the normal range or higher (Fig 6, A and B). Untreated *Rag1-F971L* mice had IgM and IgG serum levels similar to those in WT mice, and no significant changes were observed after transplantation, irrespective of the conditioning regimen used (Fig 6, A and B). Normal IgA serum levels were observed in both *Rag1*-mutant models after transplantation with use of CD45-SAP–based regimens, whereas somewhat lower levels were detected in mice conditioned with 2 Gy of irradiation (Fig 6, C). To evaluate how conditioning regimens may affect the quality of humoral immune responses after transplantation, WT and *Rag1*-mutant mice were immunized with the T-cell–dependent TNP-conjugated keyhole limpet hemocyanin antigen. Compared with untreated controls, most *Rag1*-mutant mice that received a transplant were able to produce specific antibodies, with the greatest responses being observed in CD45-SAP plus 2-Gy– and 8-Gy–treated *Rag1-KO* mice and in CD45-SAP– and 8-Gy–treated *Rag1-F971L* mice (Fig 6, D). Of note, levels of circulating autoantibodies, which are elevated in *Rag1-F971L* mice as a sign of tolerance breakdown,[24] were markedly reduced in CD45-SAP–conditioned mice and even normalized in mice conditioned with CD45-SAP plus 2 Gy of irradiation, or with 8 Gy of irradiation (see Fig E4 in the Online Repository at www.jacionline.org).

DISCUSSION

Herein, we have presented preclinical data supporting the use of a nongenotoxic, immunotoxin-based conditioning regimen for HSCT of patients with either severe or hypomorphic forms of *RAG* deficiency. We first demonstrated that in the absence of conditioning, host competition dramatically limits donor HSC engraftment, even in an MHC syngeneic setting, indicating that HSC depletion is required to allow donor cell engraftment and long-term immunologic reconstitution, irrespective of the severity of the immunologic phenotype. These findings are consistent with clinical observations. In particular, Schuetz et al have shown that unconditioned HSCT from matched sibling donors for *RAG* deficiency is associated with T-cell counts in the lower range of normal, and more variable and often incomplete, B-cell reconstitution.[7] Moreover, it has been demonstrated that *RAG* deficiency and lack of chemotherapy-based conditioning represent risk factors for incomplete immune reconstitution after HSCT from donors other than HLA-matched siblings.[5] Although a prospective clinical trial (ClinicalTrials.gov identifier NCT03619551) is currently under way to compare different doses of busulfan-based regimens for their capacity to induce immune reconstitution in newly diagnosed infants with SCID, alternative approaches, based on immunotoxins, are receiving increasing consideration, as they could help reduce the risks of acute and chronic toxicity associated with chemotherapy and TBI. In particular, promising results have been recently reported with use of antibody-drug conjugate (ADCs) for HSCT in both humanized mouse models and nonhuman primates, as well as for autologous gene therapy, and they are expected to translate soon into clinical trials.[17,28,29] These observations will be instrumental to extend a nongenotoxic regimen to patients undergoing secondary HSC transplant for loss of chimerism or insufficient thymic output.

Here, we have compared CD45-SAP immunotoxin with genotoxic TBI in terms of their capacity to permit donor stem cell engraftment and immune reconstitution in 2 mouse models of *RAG* deficiency: the *Rag1*-KO mouse, mimicking SCID,[25] and the *Rag1-F971L* mouse, modeling CID-ID.[24] A single dose of CD45-SAP immunotoxin resulted in different kinetics of LSK cells, but similar efficacy of HSC depletion in the 2 mouse models. Both in the BM and in the thymus, conditioning with 2 Gy of TBI or with CD45-SAP alone resulted in low and intermediate levels of engraftment, respectively, at pro-/pre-B and DN3 stages, in which competition from endogenous mutant cells is expected.[24,25] In contrast, combining CD45-SAP with 2 Gy of TBI had a synergistic effect, leading to more robust donor engraftment and faster kinetics of immune reconstitution in both models, similarly to what was observed with use of 8 of Gy of TBI. We also showed that CD45-SAP–based regimens allow significant improvement of thymic architecture and maturation of TECs, which support thymopoiesis and mediate positive and negative selection.[30] We had previously shown that abnormalities of thymic architecture and TEC composition in humans and mice with *RAG* defects[24,31–33] are associated with molecular signatures of self-reactivity in the peripheral T-cell repertoire.[34,35] Restoration of TEC maturation may therefore also have important implications for correction of the immune dysregulation that is often associated with RAG deficiency. Finally, conditioning of *Rag1-F971L* mice with CD45-SAP led to marked improvement of the autoantibody profile, especially when combined with low-dose

TBI, indicating that this approach allows high levels of multilineage chimerism and corrects breakdown of immune tolerance.

Besides CD45-SAP, other mAb-based regimens have also been explored as nongenotoxic conditioning regimens. In particular, a humanized anti-CD117 mAb, targeting HSPCs, is being explored as single-agent conditioning regimen in patients with SCID (ClinicalTrials.gov Identifier NCT02963064), and the safety and efficacy of CD117-SAP immunotoxin have been tested in preclinical studies.[17–19] Although targeting CD117 may open BM niches and facilitate donor stem cell engraftment,[14] this approach would not deplete more mature lymphoid cells, which may compete with donor-derived cells at later stages of T- and B-cell development. In RAG deficiency, such cells may express self-reactive specificities because of the inefficiency of negative selection and may therefore mediate immune dysregulation. Our data demonstrate that CD45-SAP can also efficiently deplete lymphoid progenitor cells and, to some degree, even more mature cells in peripheral lymphoid organs. Our data also confirm and extend previous observations[23] demonstrating the safety of this approach. A previous study has shown that a single dose of 3 mg/kg of CD45-SAP is sufficient to allow robust and durable donor engraftment.[23] In this study we have demonstrated that optimal results are achieved when combining CD45-SAP and 2 Gy of TBI. Although low-dose TBI is often used as part of conditioning regimens in humans also; nonetheless, it represents a matter of concern in infants and young children, especially in patients with genetic defects associated with increased cellular radiosensitivity. Alternative approaches, such as use of higher doses of CD45 ADCs or combination with other mAb-based conditioning agents, need to be explored and would be particularly valuable in the treatment of diseases associated with cellular radiosensitivity.

One of the limitations of CD45-SAP is its half-life, which may lead to targeting of donor-derived HSCs also if the transplantation is performed shortly after immunotoxin injection. Moreover, transient hepatotoxicity has been reported after injection of saporin alone,[22] ADCs,[17] or radiolabeled anti-CD45 antibody,[36–38] and mild signs of liver damage have also been observed in a minority of animals included in the present study. Although recent data showed that ADCs have a safer toxicity profile than do current conventional conditioning regimens based on alkylating agents and/or radiotherapy,[17] several steps are needed before advancing this type of strategy into the clinical setting. In particular, future preclinical studies, may help assess the dosage, safety, and efficacy of other anti-CD45 ADCs (CD45 ADCs) with shorter half-life and similar or even superior HSC-depleting properties.

Finally, although our model has explored the feasibility and efficacy of CD45-SAP in a mouse model of syngeneic HSCT, it is possible that more complex conditioning regimen protocols combining CD45 ADCs with other mAbs targeting T and/or natural killer cells may be needed to attain robust and durable multilineage engraftment in MHC-matched nonsyngeneic and MHC-mismatched settings.

In summary, we have demonstrated that CD45-SAP is a potent immunotoxin that can efficiently deplete endogenous HSPCs and more mature lymphoid cells, allowing robust donor stem cell engraftment and immune reconstitution in mouse models of null and hypomorphic *Rag1* mutations. These results may pave the way for applying a similar

strategy with novel CD45 ADC molecules as a conditioning regimen for HSCT or gene therapy not only in patients with RAG deficiency but also in patients with other inborn errors of immunity associated with immune dysregulation or with a higher risk of poor stem cell engraftment, reduced thymopoiesis, and premature loss of T-cell repertoire diversity after HSCT.

Supplementary Material

Refer to Web version on PubMed Central for supplementary material.

Acknowledgments

Supported by a grant from the Division of Intramural Research, National Institute of Allergy and Infectious Diseases, National Institutes of Health (to L.D.N.); the National Institutes of Health Bench to Bedside grant RAG Deficiency: From Pathophysiology to Precise Gene Editing (to L.D.N. and A.V.); and grants Tiget E2 (to A.V.), Italian Ministry of Health PE-2016-02363691 (to E.F. and L.D.N.), EU2020 (SCIDNET) No. 666908 (to A.V.), and MIUR 2017-5XHBPN (to A.V.).

Abbreviations used

ADC	Antibody drug conjugate
BM	Bone marrow
CD45-SAP	Anti-CD45 mAb conjugated with saporin
CID-ID	Combined immune deficiency with immune dysregulation
DN	Double-negative
HSC	Hematopoietic stem cell
HSCT	Hematopoietic stem cell transplantation
HSPC	Hematopoietic stem and progenitor cell
Lin$^-$	Lineage-negative
LSK	Lin$^-$ Sca1$^+$ c-kit$^+$
mTEC	Medullary thymic epithelial cell
MZ	Marginal zone
PB	Peripheral blood
RAG	Recombinase-activating gene
SCID	Severe combined immune deficiency
TBI	Total body irradiation
TEC	Thymic epithelial cell
TNP	2,4,6-Trinitrophenyl

WBC	White blood cell
WT	Wild-type

REFERENCES

1. Pai SY, Logan BR, Griffith LM, Buckley RH, Parrott RE, Dvorak CC, et al. Transplantation outcomes for severe combined immunodeficiency, 2000-2009. N Engl J Med 2014;371:434–46. [PubMed: 25075835]
2. Shearer WT, Dunn E, Notarangelo LD, Dvorak CC, Puck JM, Logan BR, et al. Establishing diagnostic criteria for severe combined immunodeficiency disease (SCID), leaky SCID, and Omenn syndrome: the Primary Immune Deficiency Treatment Consortium experience. J Allergy Clin Immunol 2014;133:1092–8. [PubMed: 24290292]
3. Picard C, Bobby Gaspar H, Al-Herz W, Bousfiha A, Casanova JL, Chatila T, et al. International Union of Immunological Societies: 2017 Primary Immunodeficiency Diseases Committee report on inborn errors of immunity. J Clin Immunol 2018;38:96–128. [PubMed: 29226302]
4. Puck JM. Newborn screening for severe combined immunodeficiency and T-cell lymphopenia. Immunol Rev 2019;287:241–52. [PubMed: 30565242]
5. Haddad EL, Logan BR, Griffith LM, Buckley RH, Parrott RE, Prockop SE, et al. SCID genotype and 6-month post-transplant CD4 count predict survival and immune recovery: a PIDTC Retrospective Study. Blood 2018;132:1737–49. [PubMed: 30154114]
6. Fischer A, Hacein-Bey-Abina S. Gene therapy for severe combined immunodeficiencies and beyond. J Exp Med 2020;217.
7. Schuetz C, Neven B, Dvorak CC, Leroy S, Ege MJ, Pannicke U, et al. SCID patients with ARTEMIS vs RAG deficiencies following HCT: increased risk of late toxicity in ARTEMIS-deficient SCID. Blood 2014;123:281–9. [PubMed: 24144642]
8. Liu A, Vosshenrich CA, Lagresle-Peyrou C, Malassis-Seris M, Hue C, Fischer A, et al. Competition within the early B-cell compartment conditions B-cell reconstitution after hematopoietic stem cell transplantation in nonirradiated recipients. Blood 2006;108:1123–8. [PubMed: 16614244]
9. Wentink MWJ, Kalina T, Perez-Andres M, Del Pino Molina L, H IJ, Kavelaars FG, et al. Delineating human B cell precursor development with genetically identified PID cases as a model. Front Immunol 2019;10:2680. [PubMed: 31849931]
10. Shaw P, Shizuru J, Hoenig M, Veys P, Iewp E. Conditioning perspectives for primary immunodeficiency stem cell transplants. Front Pediatr 2019;7:434. [PubMed: 31781522]
11. Schuetz C, Huck K, Gudowius S, Megahed M, Feyen O, Hubner B, et al. An immunodeficiency disease with RAG mutations and granulomas. N Engl J Med 2008;358:2030–8. [PubMed: 18463379]
12. Walter JE, Rosen LB, Csomos K, Rosenberg JM, Mathew D, Keszei M, et al. Broad-spectrum antibodies against self-antigens and cytokines in RAG deficiency. J Clin Invest 2016;126:4389. [PubMed: 27801680]
13. Farmer JR, Foldvari Z, Ujhazi B, De Ravin SS, Chen K, Bleesing JJH, et al. Outcomes and treatment strategies for autoimmunity and hyperinflammation in patients with RAG deficiency. J Allergy Clin Immunol Pract 2019;7:1970–85.e4. [PubMed: 30877075]
14. Czechowicz A, Kraft D, Weissman IL, Bhattacharya D. Efficient transplantation via antibody-based clearance of hematopoietic stem cell niches. Science 2007;318:1296–9. [PubMed: 18033883]
15. Xue X, Pech NK, Shelley WC, Srour EF, Yoder MC, Dinauer MC. Antibody targeting KIT as pretransplantation conditioning in immunocompetent mice. Blood 2010;116:5419–22. [PubMed: 20813896]
16. Pang WW, Czechowicz A, Logan AC, Bhardwaj R, Poyser J, Park CY, et al. Anti-CD117 antibody depletes normal and myelodysplastic syndrome human hematopoietic stem cells in xenografted mice. Blood 2019;133:2069–78. [PubMed: 30745302]

17. Czechowicz A, Palchaudhuri R, Scheck A, Hu Y, Hoggatt J, Saez B, et al. Selective hematopoietic stem cell ablation using CD117-antibody-drug-conjugates enables safe and effective transplantation with immunity preservation. Nat Commun 2019;10:617. [PubMed: 30728354]

18. Li Z, Czechowicz A, Scheck A, Rossi DJ, Murphy PM. Hematopoietic chimerism and donor-specific skin allograft tolerance after non-genotoxic CD117 antibody-drug-conjugate conditioning in MHC-mismatched allotransplantation. Nat Commun 2019;10:616. [PubMed: 30728353]

19. Gao C, Schroeder JA, Xue F, Jing W, Cai Y, Scheck A, et al. Nongenotoxic antibody-drug conjugate conditioning enables safe and effective platelet gene therapy of hemophilia A mice. Blood Adv 2019;3:2700–11. [PubMed: 31515232]

20. Krance RA, Kuehnle I, Rill DR, Mei Z, Pinetta C, Evans W, et al. Hematopoietic and immunomodulatory effects of lytic CD45 monoclonal antibodies in patients with hematologic malignancy. Biol Blood Marrow Transplant 2003;9:273–81. [PubMed: 12720220]

21. Straathof KC, Rao K, Eyrich M, Hale G, Bird P, Berrie E, et al. Haemopoietic stem-cell transplantation with antibody-based minimal-intensity conditioning: a phase 1/2 study. Lancet 2009;374:912–20. [PubMed: 19729196]

22. Polito L, Bortolotti M, Mercatelli D, Battelli MG, Bolognesi A. Saporin-S6: a useful tool in cancer therapy. Toxins (Basel) 2013;5:1698–722. [PubMed: 24105401]

23. Palchaudhuri R, Saez B, Hoggatt J, Schajnovitz A, Sykes DB, Tate TA, et al. Nongenotoxic conditioning for hematopoietic stem cell transplantation using a hematopoietic-cell-specific internalizing immunotoxin. Nat Biotechnol 2016;34:738–45. [PubMed: 27272386]

24. Ott de Bruin LM, Bosticardo M, Barbieri A, Lin SG, Rowe JH, Poliani PL, et al. Hypomorphic Rag1 mutations alter the preimmune repertoire at early stages of lymphoid development. Blood 2018;132:281–92. [PubMed: 29743177]

25. Mombaerts P, Iacomini J, Johnson RS, Herrup K, Tonegawa S, Papaioannou VE. RAG-1-deficient mice have no mature B and T lymphocytes. Cell 1992;68:869–77. [PubMed: 1547488]

26. Capo V, Castiello MC, Fontana E, Penna S, Bosticardo M, Draghici E, et al. Efficacy of lentivirus-mediated gene therapy in an Omenn syndrome recombination-activating gene 2 mouse model is not hindered by inflammation and immune dysregulation. J Allergy Clin Immunol 2018;142:928–41.e8. [PubMed: 29241731]

27. Bosticardo M, Yamazaki Y, Cowan J, Giardino G, Corsino C, Scalia G, et al. Heterozygous FOXN1 variants cause low TRECs and severe T cell lymphopenia, revealing a crucial role of FOXN1 in supporting early thymopoiesis. Am J Hum Genet 2019;105:549–61. [PubMed: 31447097]

28. Pearse BR, McDonough SM, Proctor JL, Panwar R, Sarma GN, Kien L, et al. A CD117-amanitin antibody drug conjugate (ADC) effectively depletes human and non-human primate hematopoietic stem and progenitor cells (HSPCs): targeted non-genotoxic conditioning for bone marrow transplant. Biol Blood Marrow Transplant 2019;25:S29–30.

29. Tisdale JF, Donahue RE, Uchida N, Pearse BR, McDonough SM, Proctor JL, et al. A single dose of CD117 antibody drug conjugate enables autologous gene-modified hematopoietic stem cell transplant (gene therapy) in nonhuman primates. Blood 2019;134(S1):610.

30. Kadouri N, Nevo S, Goldfarb Y, Abramson J. Thymic epithelial cell heterogeneity: TEC by TEC. Nat Rev Immunol 2020;20:239–53. [PubMed: 31804611]

31. Poliani PL, Facchetti F, Ravanini M, Gennery AR, Villa A, Roifman CM, et al. Early defects in human T-cell development severely affect distribution and maturation of thymic stromal cells: possible implications for the pathophysiology of Omenn syndrome. Blood 2009;114:105–8. [PubMed: 19414857]

32. Marrella V, Poliani PL, Notarangelo LD, Grassi F, Villa A. Rag defects and thymic stroma: lessons from animal models. Front Immunol 2014;5:259. [PubMed: 25076946]

33. De Ravin SS, Cowen EW, Zarember KA, Whiting-Theobald NL, Kuhns DB, Sandler NG, et al. Hypomorphic Rag mutations can cause destructive midline granulomatous disease. Blood 2010;116:1263–71. [PubMed: 20489056]

34. Rowe JH, Stadinski BD, Henderson LA, de Bruin LO, Delmonte O, Lee YN, et al. Abnormalities of T-cell receptor repertoire in CD4(+) regulatory and conventional T cells in patients with RAG

mutations: implications for autoimmunity. J Allergy Clin Immunol 2017;140:1739–43.e7. [PubMed: 28864286]

35. Daley SR, Koay HF, Dobbs K, Bosticardo M, Wirasinha RC, Pala F, et al. Cysteine and hydrophobic residues in CDR3 serve as distinct T-cell self-reactivity indices. J Allergy Clin Immunol 2019;144:333–6. [PubMed: 31053347]
36. Burtner CR, Chandrasekaran D, Santos EB, Beard BC, Adair JE, Hamlin DK, et al. (211)Astatine-conjugated monoclonal CD45 antibody-based nonmyeloablative conditioning for stem cell gene therapy. Hum Gene Ther 2015;26:399–406. [PubMed: 25919226]
37. Nakamae H, Wilbur DS, Hamlin DK, Thakar MS, Santos EB, Fisher DR, et al. Biodistributions, myelosuppression, and toxicities in mice treated with an anti-CD45 antibody labeled with the α-emitting radionuclides bismuth-213 or astatine-211. Cancer Res 2009;69:2408–15. [PubMed: 19244101]
38. Chen Y, Kornblit B, Hamlin DK, Sale GE, Santos EB, Wilbur DS, et al. Durable donor engraftment after radioimmunotherapy using α-emitter astatine-211–labeled anti-CD45 antibody for conditioning in allogeneic hematopoietic cell transplantation. Blood 2012;119:1130–8. [PubMed: 22134165]

Clinical implications:

Conditioning with anti-CD45 ADCs may represents a novel and safe conditioning regimen for patients with *RAG* deficiency and other inborn errors of immunity.

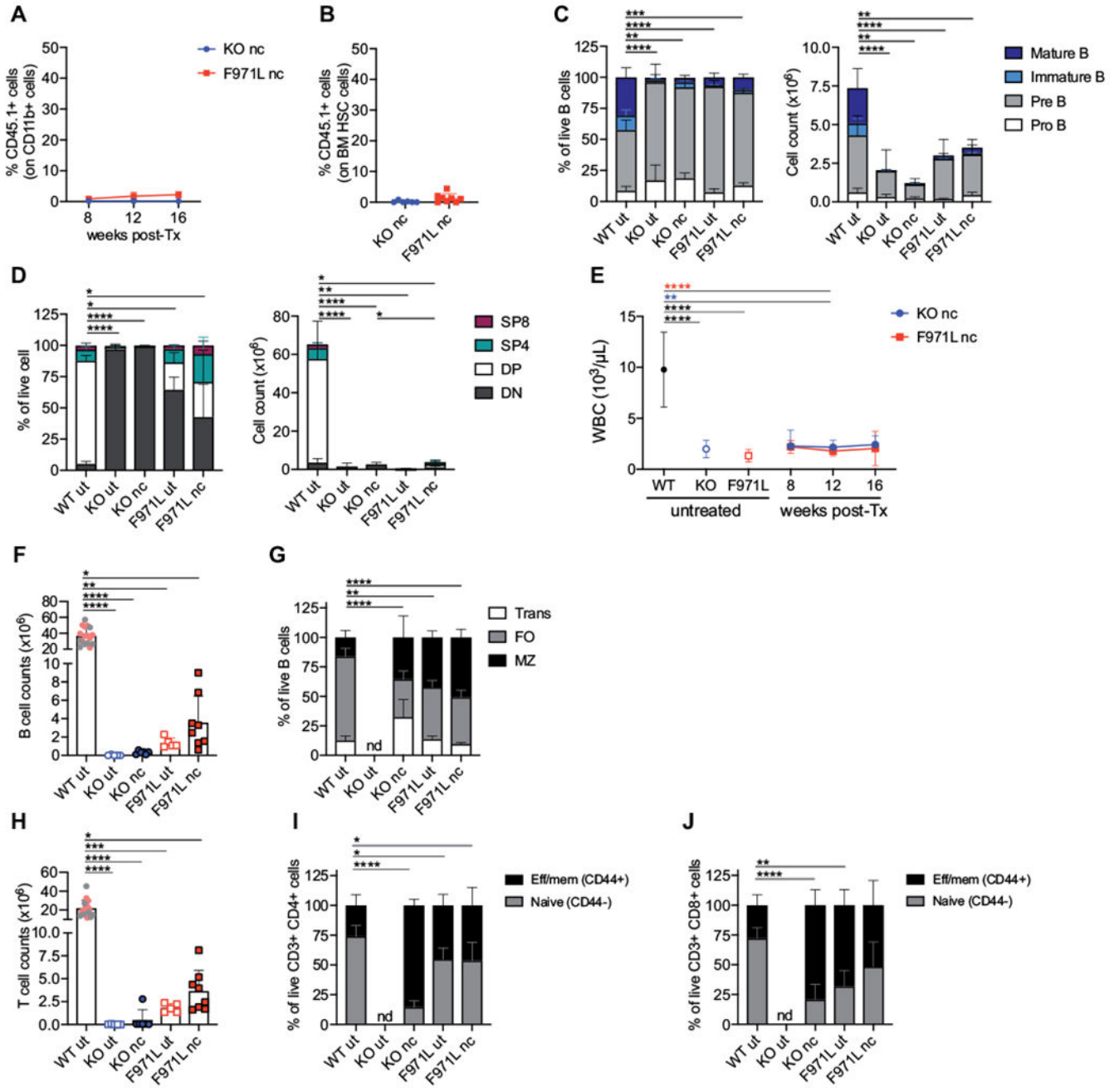

FIG 1.

Myeloid chimerism and immunologic reconstitution in unconditioned *Rag1*^{mut} mice. **A**, Kinetics of myeloid chimerism measured by flow cytometry as the proportion of donor WT CD45.1^{+} cells gated on CD11b^{+} cells in the peripheral blood at different time points after the transplant (post-Tx) in nonconditioned (nc) *Rag1-KO* (knockout [KO]) mice (n = 6) and *Rag1-F971L* (F971L) mice (n = 5-9). **B**, Donor chimerism in HSCs identified as LSK CD150^{+}CD48^{-} cells of Lin^{-} cells isolated from BM cells 16 weeks after the transplant. **C**, B-cell developmental stages were analyzed by flow cytometry in untreated (ut) mice or 16 weeks after transplant in nc mice and shown as proportion (*left panel*) and absolute counts

(*right panel*) of B cells in BM (WT [n = 23], KO ut [n = 9], KO nc [n = 6], F971L ut [n = 5], and F971L nc [n = 8] mice). One-way ANOVA, Kruskal-Wallis test on pre–B-cell frequencies (*left panel*) and immature B-cell counts (*right panel*). **D**, $CD4^{-}CD8^{-}$ double-negative (DN), $CD4^{+}CD8^{+}$ double-positive, SP4 ($CD4^{+}CD8^{-}$), and SP8 ($CD4^{-}CD8^{+}$) cells were analyzed by flow cytometry and shown as proportion of thymocytes (*left panel*) and absolute counts (*right panel*) (WT [n = 20], KO ut [n = 7], KO nc [n = 6], F971L ut [n = 5], and F971L nc [n = 8] mice). One-way ANOVA, Kruskal-Wallis test on DN cell frequencies (*left panel*) and double-positive (DP) cell counts (*right panel*). **E**, WBCs were measured over time in the PB. One-way ANOVA, Kruskal-Wallis test at 12 weeks after the transplant. Asterisk colors indicate the groups of comparison. **F**, Splenic B-cell counts are shown in the graph. **G**. Proportions of splenic transitional (Trans), follicular (FO), and MZ B cells were analyzed by flow cytometry. One-way ANOVA, Kruskal-Wallis test on FO B-cell frequencies. **H**, Splenic T-cell counts are shown in the graph. **I** and **J**, Phenotypic analysis results of splenic T lymphocytes are shown in the graph according to the expression of CD44 on the $CD3^{+}CD4^{+}$ cells (**I**) and $CD3^{+}CD8^{+}$ cells (**J**); 1-way ANOVA, Kruskal-Wallis test on naive T cells. **F** and **H**, Gray dots in WT bar were values from the SR-Tiget laboratory, and pink dots indicate values from the National Institutes of Health laboratory; 1-way ANOVA, Kruskal-Wallis test for multiple comparison. $*P < .05$; $**P < .005$; $***P < .0005$; $****P < .0001$. Means ± SDs are shown. *Eff/mem*, Effector/memory.

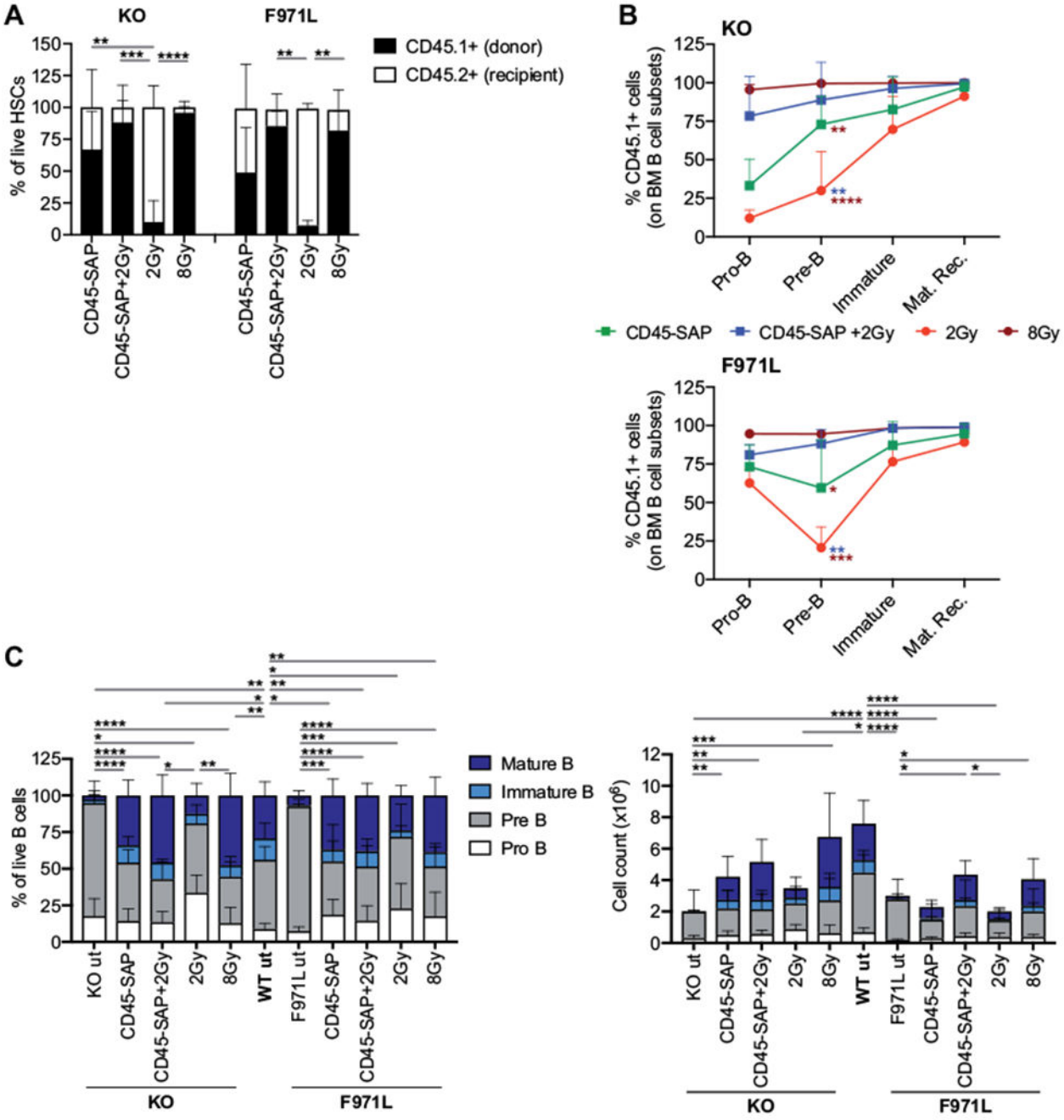

FIG 2.

Donor chimerism and immunologic reconstitution in the BM of conditioned *Rag1*^{mut} mice. **A**, Donor chimerism in HSCs was measured by flow cytometry in Lin^{-} cells isolated from *Rag1-KO* (knockout [KO]) and *Rag1-F971L* (F971L) mice and shown as the proportion of donor CD45.1^{+} cells and recipient CD45.2^{+} cells in an LSK CD150^{+}CD48^{-} cell gate. One-way ANOVA, Krustal-Wallis test for multiple comparison. **B**, The proportion of CD45.1^{+} donor WT cells was evaluated in the main stages of B-cell development in the BM of *Rag1-KO* (*top panel*) and *Rag1-F971L* (*bottom panel*) mice. One-way ANOVA, Kruskal-Wallis

test on pre–B-cell frequencies. Asterisk colors indicate the groups of comparison. **C**, The B-cell developmental stages were analyzed by flow cytometry and shown as proportion (*left panel*) and absolute counts (*right panel*) of B cells in the BM. One-way ANOVA, Kruskal-Wallis test on pre–B-cell frequencies (*left panel*) and immature B-cell counts (*right panel*). **A-C**, Analyses were performed 16 weeks after the transplant. $*P < .05$; $**P < .005$; $***P < .0005$; $****P < .0001$. Means ± SDs are shown. *mat. rec.*, Mature recirculating; *ut*, untreated.

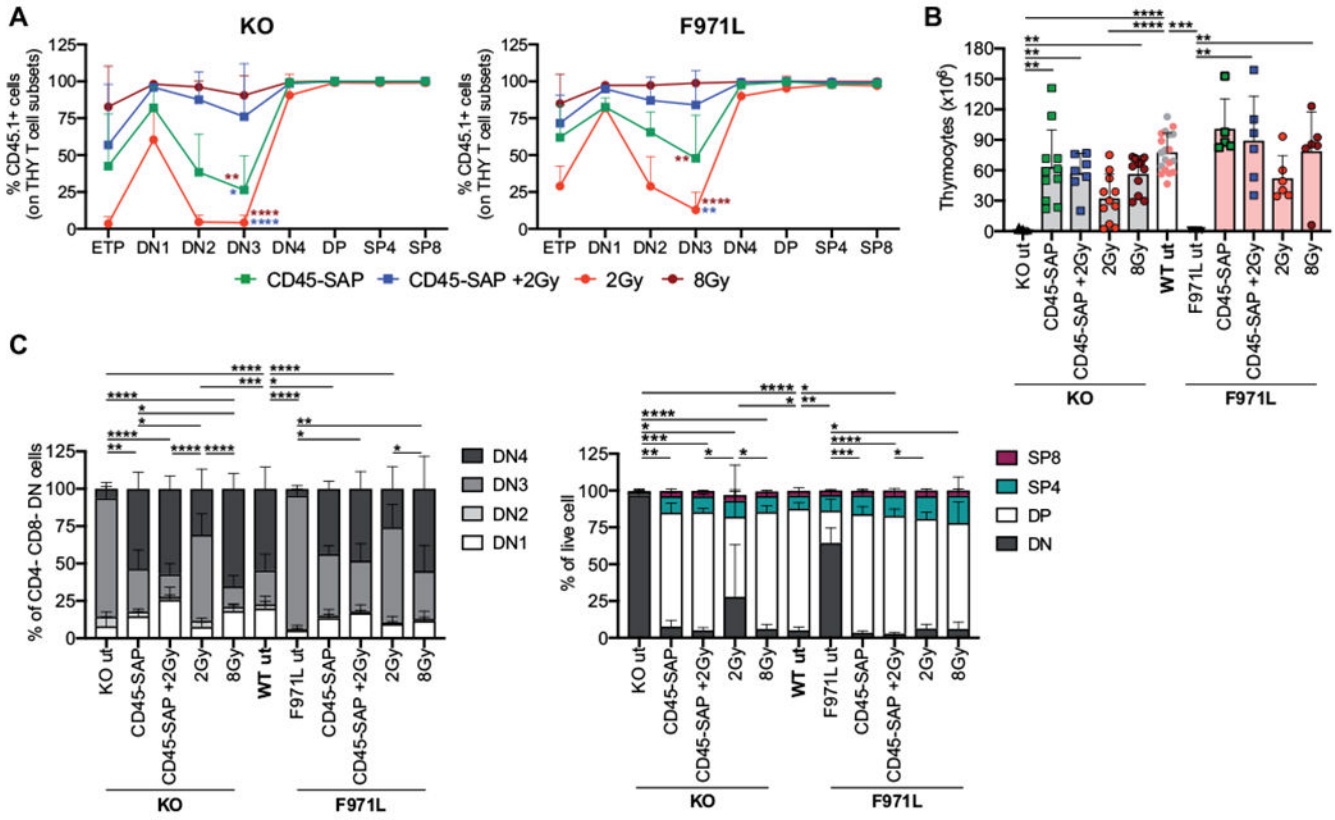

FIG 3.

Donor chimerism and reconstitution in the thymus of conditioned *Rag1*^{mut} mice. **A**, Donor contribution during thymopoiesis of *Rag1-KO* (KO) and *Rag1-F971L* (F971L) mice is shown as proportion of donor WT CD45.1^{+} cells measured in each developmental stage: early thymic progenitor (Lin^{-}CD8^{-}CD25^{-}cKit^{+}CD44^{-}), double-negative (DN) (DN1 [CD4^{-}CD8^{-}CD25^{-}CD44^{+}], DN2 [CD4^{-}CD8^{-}CD25^{+}CD44^{+}], DN3 [CD4^{-}CD8^{-}CD25^{+}CD44^{-}], DN4 [CD4^{-}CD8^{-}CD25^{-}CD44^{-}], double-positive (DP) (CD4^{+}CD8^{+}), SP4 (CD4^{+}CD8^{-}), and SP8 (CD4^{-}CD8^{+}) cells. One-way ANOVA, Kruskal-Wallis test on DN3 cell frequencies. Asterisk colors indicate the groups of comparison. **B**, Total cell counts in the thymus are shown. For WT untreated mice (wt ut), gray and pink dots in the bar represent values obtained at SR-Tiget and at the National Institutes of Health, respectively. One-way ANOVA, Kruskal-Wallis test for multiple comparison. C, Subset distribution of developing T cells was assessed by flow cytometry. One-way ANOVA, Kruskal-Wallis test for multiple comparison on DN3 cell (*left panel*) or DN cell (*right panel*) frequencies. A-C, Analyses were performed 16 weeks after the transplant. *P < .05; **P < .005; ***P < .0005; ****P < .0001. Means ± SDs are shown. *THY*, Thymocytes.

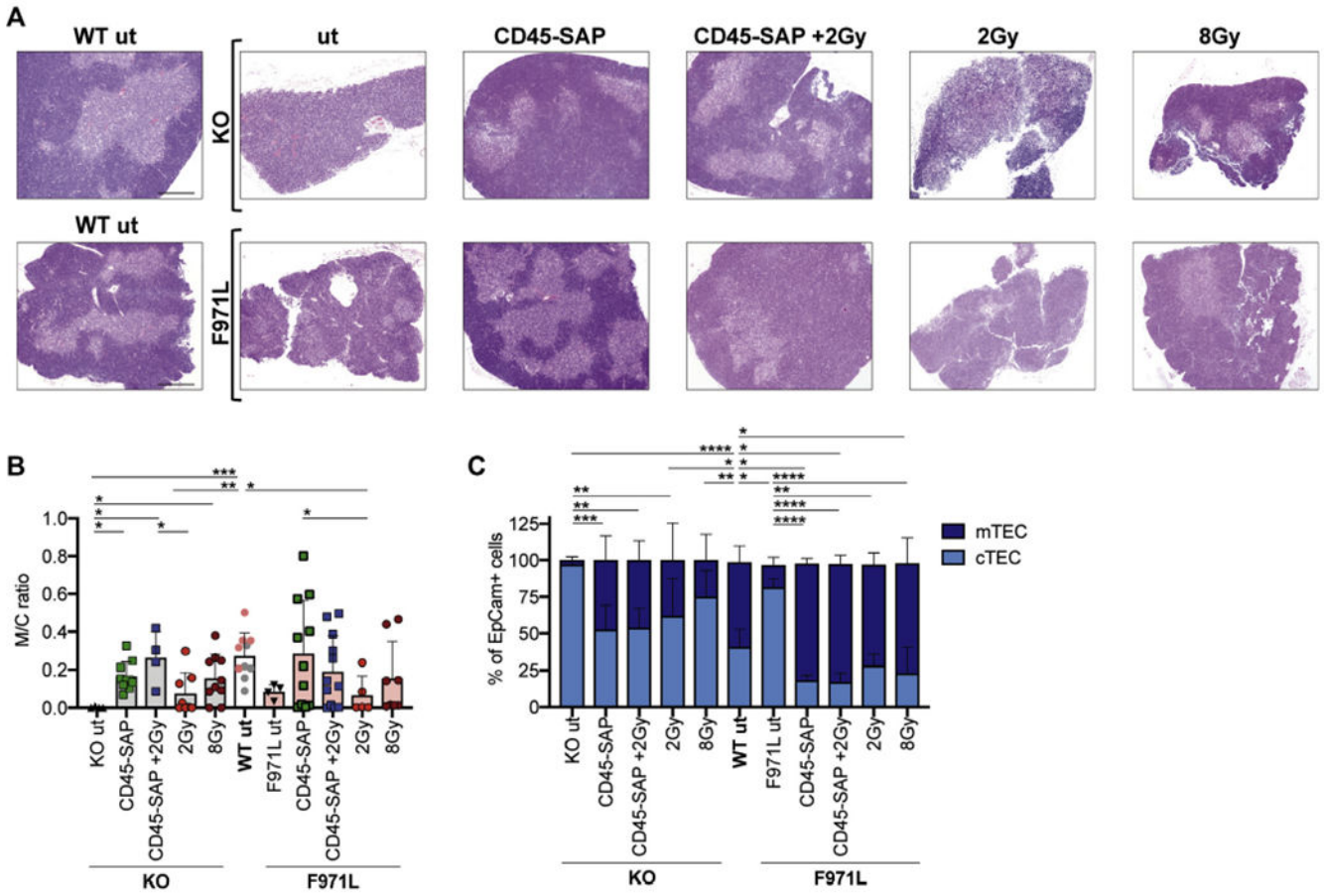

FIG 4.

TEC reconstitution in conditioned *Rag1*^{mut} mice. **A**, Representative images of thymic sections stained with hematoxylin and eosin (4*x* objective and 500-μm scale bar). **B**, Medullary (M) and cortical (C) areas were measured on thymic sections stained with hematoxylin and eosin and shown as a ratio. Gray dots in the WT bar are values from the SR-Tiget laboratory, and pink dots are values from the from the NIH laboratory; 1-way ANOVA, Kruskal-Wallis test for multiple comparison. **C**, TEC reconstitution was measured as the proportion of mTECs (EpCam+ Ly51^{+} UEA1^{high}/CD80^{high}) and cortical TECs (EpCam^{+} Ly51^{+} UEA1^{low}/CD80^{low}) were measured by flow cytometry 16 weeks after the transplant in *Rag1*-KO (knockout [KO] and *Rag1*-F971L [F971L] mice. One-way ANOVA, Kruskal-Wallis test for multiple comparison was applied on mTEC frequencies. *P < .05; **P < .005; ***P < .0005; ****P < .0001. Means ± SDs are shown.

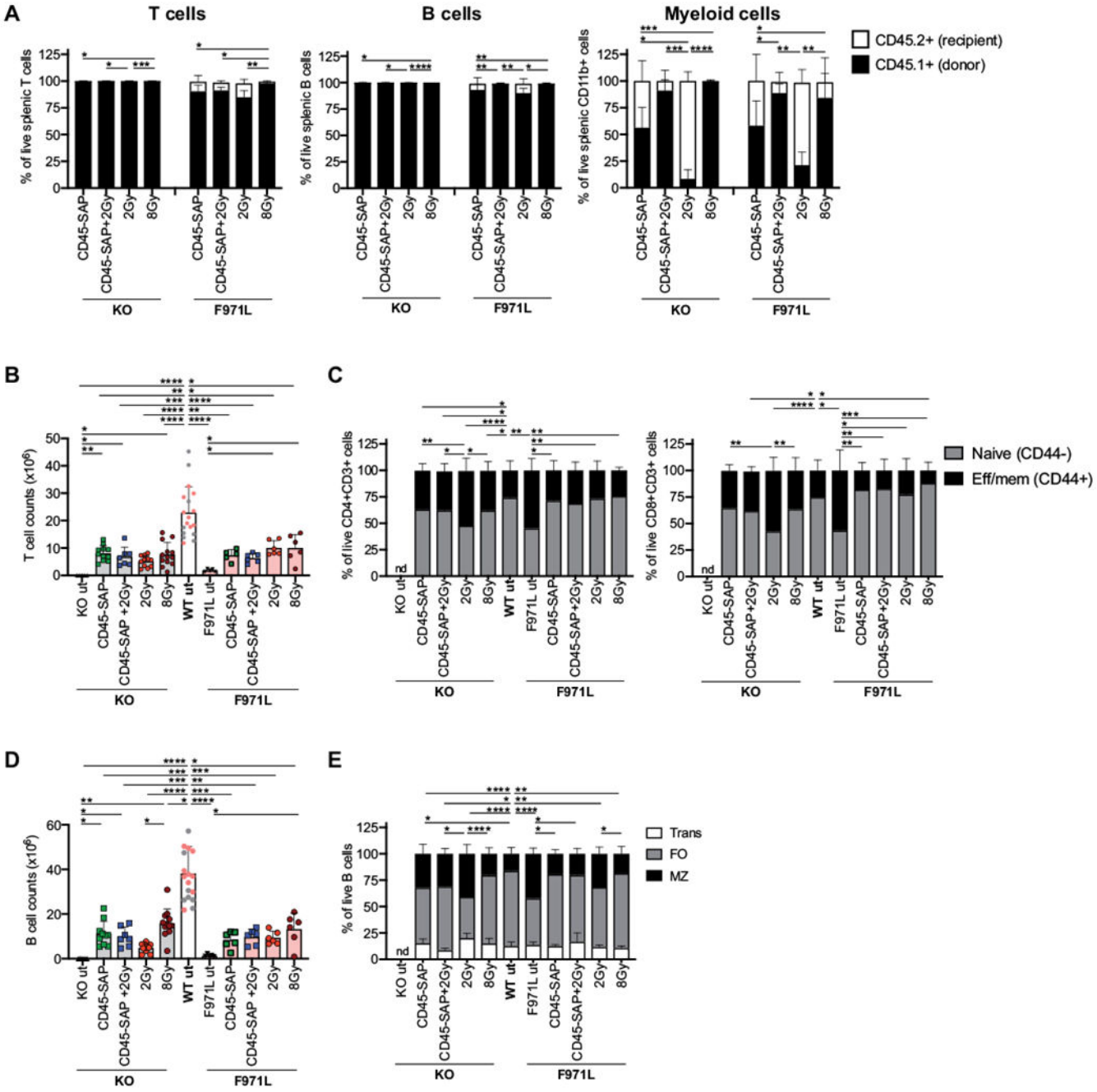

FIG 5.

Donor chimerism and reconstitution in the spleen of conditioned *Rag1*^{mut} mice. **A**, Donor chimerism in T (CD3$^+$), B (CD19$^+$ B220$^+$), and myeloid (CD11b$^+$ B220$^-$) cells was measured by flow cytometry in splenocytes isolated from *Rag1-KO* (KO) and *Rag1-F971L* (F971L) mice and shown as proportion of donor CD45.1$^+$ cells and recipient CD45.2$^+$ cells; 1-way ANOVA, Kruskal-Wallis test for multiple comparison on CD45.1$^+$ cell frequencies. **B**, Splenic T-cell counts are shown. **C**, Phenotypic analysis results of splenic T lymphocytes were evaluated according to the expression of CD44 in the CD3$^+$CD4$^+$ (*left panel*) and

$CD8^+$ cells (*right panel*); 1-way ANOVA, Kruskal-Wallis test for multiple comparison on naive T-cell frequencies. **D**, Splenic B-cell counts are shown. **E**, B-cell subsets' distribution in spleen was evaluated as proportion of transitional (Trans), follicular (FO), and MZ B cells, as analyzed by flow cytometry. One-way ANOVA, Kruskal-Wallis test on FO B-cell frequencies. **B** and **D**, One-way ANOVA, Kruskal-Wallis test for multiple comparison. **A-E**, Analyses were performed 16 weeks after the transplant. $*P < .05$; $**P < .005$; $***P < .0005$; $****P < .0001$. Means ± SDs are shown. *Eff/mem*, Effector/memory.

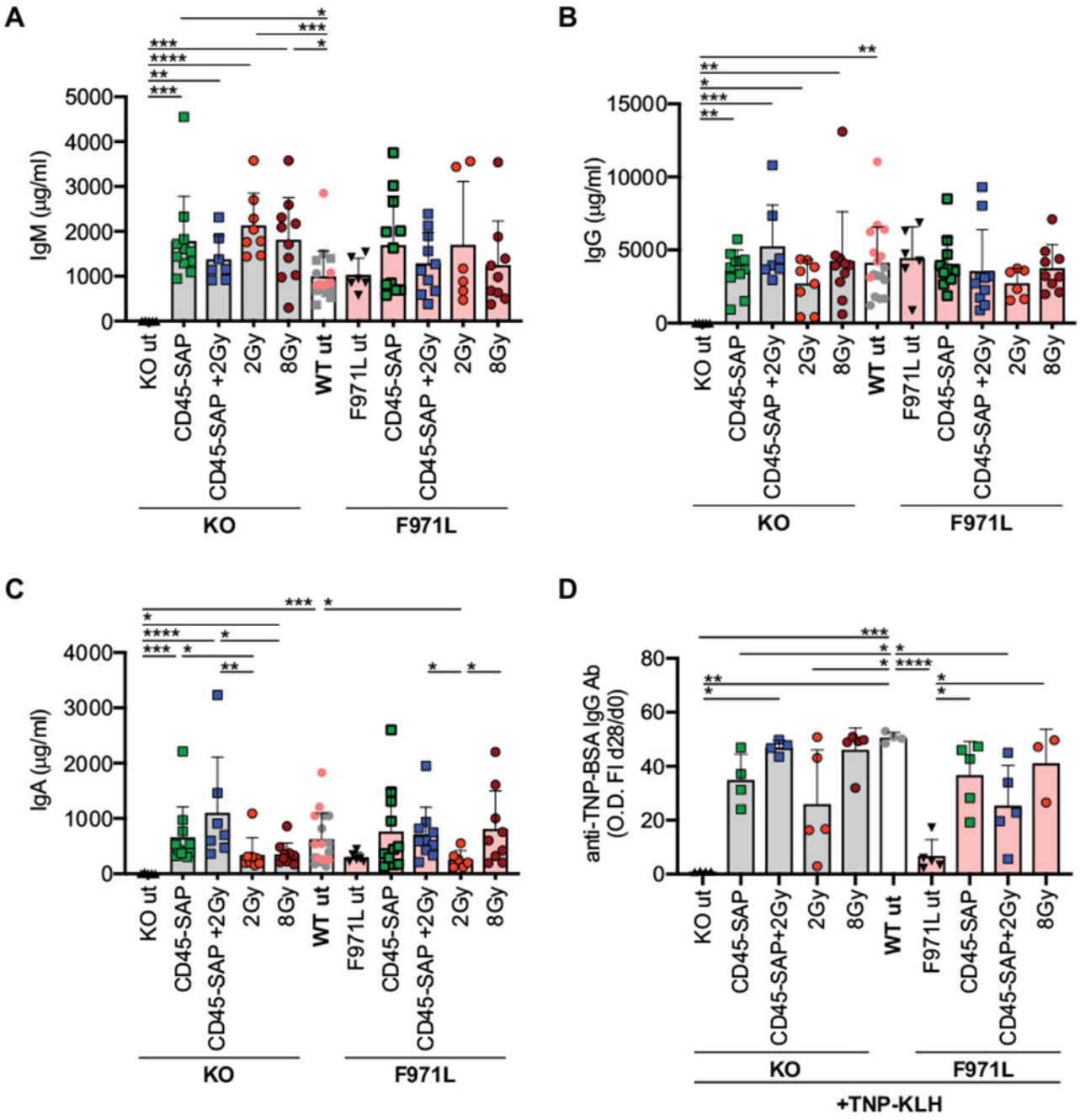

FIG 6.

In vivo immune cell function of conditioned *Rag1*^{mut} mice. **A-C**, Immunoglobulin (Ig) levels were analyzed in plasma of *Rag1*^{mut} mice 16 weeks after the transplant. **D**, *In vivo* T-cell–dependent response was measured as anti–TNP-BSA IgG levels in the plasma of *Rag1*^{mut} mice 28 days after the first TNP-conjugated keyhole limpet hemocyanin (TNP-KLH) challenge by ELISA, and the specific response was shown as fold increase (FI) between the OD values at day 28 versus at day 0 (before challenge). **A-D**, One-way

ANOVA, Kruskal-Wallis test for multiple comparison. *$P < .05$; **$P < .005$; ***$P < .0005$; ****$P < .0001$. Means ± SDs are shown. *Ab*, Antibody.